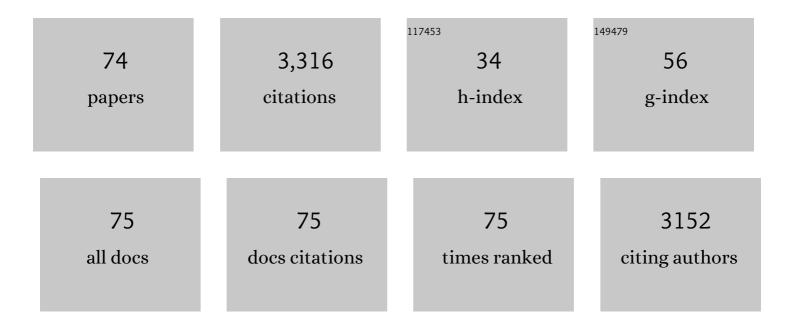
List of Publications by Year in descending order

Source: https://exaly.com/author-pdf/7978736/publications.pdf Version: 2024-02-01



#	Article	IF	CITATIONS
1	Advances in application of g–C3N4–based materials for treatment of polluted water and wastewater via activation of oxidants and photoelectrocatalysis: A comprehensive review. Chemosphere, 2022, 286, 131737.	4.2	50
2	Metal ion recovery from electrodialysis-concentrated plating wastewater via pilot-scale sequential electrowinning/chemical precipitation. Journal of Cleaner Production, 2022, 330, 129879.	4.6	37
3	Surface modification of polypropylene non-woven filter by O2 plasma/acrylic acid enhancing Prussian blue immobilization for aqueous cesium adsorption. Applied Surface Science, 2022, 590, 153101.	3.1	12
4	Current and future trends in adsorption for environmental separations. Journal of Hazardous Materials, 2022, 433, 128776.	6.5	3
5	Adsorption of Chromate Ions by Layered Double Hydroxide–Bentonite Nanocomposite for Groundwater Remediation. Nanomaterials, 2022, 12, 1384.	1.9	8
6	Quasi-Solid-State SiO2 Electrolyte Prepared from Raw Fly Ash for Enhanced Solar Energy Conversion. Materials, 2022, 15, 3576.	1.3	1
7	Particle size and interlayer anion effect on chromate adsorption by MgAl-layered double hydroxide. Applied Clay Science, 2022, 225, 106552.	2.6	12
8	Unveiling the positive effect of mineral induced natural organic matter (NOM) on catalyst properties and catalytic dechlorination performance: An experiment and DFT study. Water Research, 2022, 222, 118871.	5.3	3
9	The role of Fe dissolution in olivine-hydroxylamine-induced Fenton reaction for enhanced oxidative degradation of organic pollutant. Chemosphere, 2022, 306, 135557.	4.2	5
10	Differential contribution of excitatory and inhibitory neurons in shaping neurovascular coupling in different epileptic neural states. Journal of Cerebral Blood Flow and Metabolism, 2021, 41, 1145-1161.	2.4	13
11	Characterization of rare earth elements present in coal ash by sequential extraction. Journal of Hazardous Materials, 2021, 402, 123760.	6.5	50
12	Competitive adsorption of pharmaceuticals in lake water and wastewater effluent by pristine and NaOH-activated biochars from spent coffee wastes: Contribution of hydrophobic and Ĭ€-Ï€ interactions. Environmental Pollution, 2021, 270, 116244.	3.7	84
13	The enhanced reduction of bromate by highly reactive and dispersive green nano-zerovalent iron (G-NZVI) synthesized with onion peel extract. RSC Advances, 2021, 11, 5008-5018.	1.7	7
14	Fenton oxidation of synthetic food dyes by Fe-embedded coffee biochar catalysts prepared at different pyrolysis temperatures: A mechanism study. Chemical Engineering Journal, 2021, 421, 129943.	6.6	44
15	Upcycling of steel slag for manufacture of Prussian-blue-encapsulated pectin beads and its use for efficient removal of aqueous cesium. Journal of Cleaner Production, 2021, 319, 128786.	4.6	9
16	Carbon-Neutrality in Wastewater Treatment Plants: Advanced Technologies for Efficient Operation and Energy/Resource Recovery. Energies, 2021, 14, 8514.	1.6	10
17	Advances in the catalytic reduction of nitrate by metallic catalysts for high efficiency and N2 selectivity: A review. Chemical Engineering Journal, 2020, 384, 123252.	6.6	92
18	Synergistic effect of Cu loading on Fe sites of fly ash for enhanced catalytic reduction of nitrophenol. Science of the Total Environment, 2020, 705, 134544.	3.9	22

#	Article	IF	CITATIONS
19	Effects of vertical and horizontal configurations of different numbers of brush anodes on performance and electrochemistry of microbial fuel cells. Journal of Cleaner Production, 2020, 277, 124125.	4.6	43
20	Roll-to-roll production of a cellulose filter with immobilized Prussian blue for 137Cs adsorption. Journal of Environmental Chemical Engineering, 2020, 8, 104273.	3.3	5
21	Adsorption capacity of the corrosion products of nanoscale zerovalent iron for emerging contaminants. Environmental Science: Nano, 2020, 7, 3773-3782.	2.2	6
22	Enhanced denitrification of contaminated groundwater by novel bimetallic catalysts supported on kaolin-derived zeolite: effects of natural dissolved inorganic and organic matter. Environmental Science: Nano, 2020, 7, 3965-3978.	2.2	7
23	Exploring reductive degradation of fluorinated pharmaceuticals using Al2O3-supported Pt-group metallic catalysts: Catalytic reactivity, reaction pathways, and toxicity assessment. Water Research, 2020, 185, 116242.	5.3	21
24	Highly fast and selective removal of nitrate in groundwater by bimetallic catalysts supported by fly ash-derived zeolite Na-X. Environmental Science: Nano, 2020, 7, 3360-3371.	2.2	8
25	Effect of groundwater ions (Ca2+, Na+, and HCO3â^') on removal of hexavalent chromium by Fe(II)-phosphate mineral. Journal of Hazardous Materials, 2020, 398, 122948.	6.5	15
26	Red mud-activated peroxymonosulfate process for the removal of fluoroquinolones in hospital wastewater. Water Research, 2020, 184, 116171.	5.3	35
27	Support induced influence on the reactivity and selectivity of nitrate reduction by Sn-Pd bimetallic catalysts. Journal of Environmental Chemical Engineering, 2020, 8, 103754.	3.3	7
28	Development of biocatalysts immobilized on coal ash-derived Ni-zeolite for facilitating 4-chlorophenol degradation. Bioresource Technology, 2020, 307, 123201.	4.8	12
29	Nitrate reduction on surface of Pd/Sn catalysts supported by coal fly ash-derived zeolites. Journal of Hazardous Materials, 2019, 374, 309-318.	6.5	39
30	Surface modification of poly(vinyl alcohol) sponge by acrylic acid to immobilize Prussian blue for selective adsorption of aqueous cesium. Chemosphere, 2019, 226, 173-182.	4.2	44
31	Prussian blue immobilized cellulosic filter for the removal of aqueous cesium. Science of the Total Environment, 2019, 670, 779-788.	3.9	37
32	Highly efficient and magnetically recyclable Pd catalyst supported by iron-rich fly ash@fly ash-derived SiO2 for reduction of p-nitrophenol. Journal of Hazardous Materials, 2019, 371, 72-82.	6.5	38
33	Development of magnetically separable Cu catalyst supported by pre-treated steel slag. Korean Journal of Chemical Engineering, 2019, 36, 1814-1825.	1.2	6
34	Enhanced removal of antibiotics in hospital wastewater by Fe–ZnO activated persulfate oxidation. Environmental Science: Water Research and Technology, 2019, 5, 2193-2201.	1.2	15
35	Preparation of quasi-solid-state electrolytes using a coal fly ash derived zeolite-X and -A for dye-sensitized solar cells. Journal of Industrial and Engineering Chemistry, 2019, 71, 378-386.	2.9	25
36	Novel synthesis of nanoscale zerovalent iron from coal fly ash and its application in oxidative degradation of methyl orange by Fenton reaction. Journal of Hazardous Materials, 2019, 365, 751-758.	6.5	39

#	Article	IF	CITATIONS
37	Immobilization of uranium(VI) in a cementitious matrix with nanoscale zerovalent iron (NZVI). Chemosphere, 2019, 215, 626-633.	4.2	22
38	Fabrication of Ti/Ir-Ru electrode by spin coating method for electrochemical removal of copper. Environmental Engineering Research, 2019, 24, 646-653.	1.5	14
39	Novel bimetallic catalyst supported by red mud for enhanced nitrate reduction. Chemical Engineering Journal, 2018, 348, 877-887.	6.6	67
40	Exploring the complex removal behavior of natural organic matter upon N-doped reduced graphene oxide-activated persulfate via excitation-emission matrix combined with parallel factor analysis and size exclusion chromatography. Chemical Engineering Journal, 2018, 347, 252-262.	6.6	16
41	Formation of Fe nanoparticles on water-washed coal fly ash for enhanced reduction of p-nitrophenol. Chemosphere, 2018, 202, 733-741.	4.2	30
42	Immobilization and characterization of Fe(0) catalyst on NaOH-treated coal fly ash for catalytic reduction of p-nitrophenol. Chemosphere, 2018, 212, 1020-1029.	4.2	19
43	Advances in Surface Passivation of Nanoscale Zerovalent Iron: A Critical Review. Environmental Science & Technology, 2018, 52, 12010-12025.	4.6	225
44	Molecular Identification of Cr(VI) Removal Mechanism on Vivianite Surface. Environmental Science & Technology, 2018, 52, 10647-10656.	4.6	53
45	Reductive dechlorination of carbon tetrachloride by bioreduction of nontronite. Journal of Hazardous Materials, 2017, 334, 104-111.	6.5	13
46	New Features and Uncovered Benefits of Polycrystalline Magnetite as Reusable Catalyst in Reductive Chemical Conversion. Journal of Physical Chemistry C, 2017, 121, 25195-25205.	1.5	15
47	Reductive dechlorination of trichloroethylene by polyvinylpyrrolidone stabilized nanoscale zerovalent iron particles with Ni. Journal of Hazardous Materials, 2017, 340, 399-406.	6.5	40
48	Degradation of 17α-ethinylestradiol by nano zero valent iron under different pH and dissolved oxygen levels. Water Research, 2017, 125, 32-41.	5.3	45
49	Removal of nitrate by electrodialysis: effect of operation parameters. Membrane Water Treatment, 2017, 8, 201-210.	0.5	7
50	Effect of promoter and noble metals and suspension pH on catalytic nitrate reduction by bimetallic nanoscale Fe <sup>0</sup> catalysts. Environmental Technology (United Kingdom), 2016, 37, 1077-1087.	1.2	18
51	Synergistic effect of nano-sized mackinawite with cyano-cobalamin in cement slurries for reductive dechlorination of tetrachloroethylene. Journal of Hazardous Materials, 2016, 311, 1-10.	6.5	14
52	Effect of NaBH 4 on properties of nanoscale zero-valent iron and its catalytic activity for reduction of p -nitrophenol. Applied Catalysis B: Environmental, 2016, 182, 541-549.	10.8	229
53	Flavin mononucleotide mediated microbial fuel cell in the presence of Shewanella putrefaciens CN32 and iron-bearing mineral. Biotechnology and Bioprocess Engineering, 2015, 20, 894-900.	1.4	12
54	Theoretical and Experimental Studies of the Dechlorination Mechanism of Carbon Tetrachloride on a Vivianite Ferrous Phosphate Surface. Journal of Physical Chemistry A, 2015, 119, 5714-5722.	1.1	14

#	Article	IF	CITATIONS
55	Catalytic Nitrate Removal in Continuous Bimetallic Cu–Pd/Nanoscale Zerovalent Iron System. Industrial & Engineering Chemistry Research, 2015, 54, 6247-6257.	1.8	78
56	Reactivity of Nanoscale Zero-Valent Iron in Unbuffered Systems: Effect of pH and Fe(II) Dissolution. Environmental Science & Technology, 2015, 49, 10536-10543.	4.6	137
57	Degradation of pyrene in cetylpyridinium chloride-aided soil washing wastewater by pyrite Fenton reaction. Chemical Engineering Journal, 2014, 249, 34-41.	6.6	53
58	Nitrite Reduction Mechanism on a Pd Surface. Environmental Science & Technology, 2014, 48, 12768-12774.	4.6	188
59	Development of Pd–Cu/Hematite Catalyst for Selective Nitrate Reduction. Environmental Science & Technology, 2014, 48, 9651-9658.	4.6	150
60	Degradation of off-gas toluene in continuous pyrite Fenton system. Journal of Hazardous Materials, 2014, 280, 31-37.	6.5	38
61	Influence of Riboflavin on Nanoscale Zero-Valent Iron Reactivity during the Degradation of Carbon Tetrachloride. Environmental Science & Technology, 2014, 48, 2368-2376.	4.6	83
62	Riboflavin-mediated RDX transformation in the presence of Shewanella putrefaciens CN32 and lepidocrocite. Journal of Hazardous Materials, 2014, 274, 24-31.	6.5	17
63	Degradation of diclofenac by pyrite catalyzed Fenton oxidation. Applied Catalysis B: Environmental, 2013, 134-135, 93-102.	10.8	320
64	The effect of pH and zwitterionic buffers on catalytic nitrate reduction by TiO2-supported bimetallic catalyst. Chemical Engineering Journal, 2013, 232, 327-337.	6.6	51
65	Biotransformation of lepidocrocite in the presence of quinones and flavins. Geochimica Et Cosmochimica Acta, 2013, 114, 144-155.	1.6	39
66	Formation of surface mediated iron colloids during U(VI) and nZVI interaction. Advances in Environmental Research, 2013, 2, 167-177.	0.3	15
67	Adsorption of cationic cetylpyridinium chloride on pyrite surface. Journal of Industrial and Engineering Chemistry, 2012, 18, 1482-1488.	2.9	34
68	Enhanced reductive degradation of carbon tetrachloride by biogenic vivianite and Fe(II). Geochimica Et Cosmochimica Acta, 2012, 85, 170-186.	1.6	43
69	Nitrate reduction by maghemite supported Cu-Pd bimetallic catalyst. Applied Catalysis B: Environmental, 2012, 127, 148-158.	10.8	99
70	Degradation of carbon tetrachloride in modified Fenton reaction. Korean Journal of Chemical Engineering, 2012, 29, 769-774.	1.2	12
71	Enhanced Degradation of TNT and RDX by Bio-reduced Iron Bearing Soil Minerals. Advances in Environmental Research, 2012, 1, 1-14.	0.3	22
72	Degradation of trichloroethylene by Fenton reaction in pyrite suspension. Journal of Hazardous Materials, 2011, 185, 1355-1361.	6.5	143

#	Article	IF	CITATIONS
73	Inhibition of nZVI reactivity by magnetite during the reductive degradation of 1,1,1-TCA in nZVI/magnetite suspension. Applied Catalysis B: Environmental, 2010, 96, 10-17.	10.8	74
74	Selective reduction of highly concentrated nitrate by electrochemical method using a combination of Zn and Ti/Ir-Ru electrodes. , 0, 95, 186-191.		2